CRP TIME MIGRATION

T. A. Coimbra, J. H. Faccipieri, and M. Tygel

email: *tgo.coimbra@gmail.com, jorge.faccipieri@gmail.com, tygel@ime.unicamp.br*
keywords: *Common Reflection Point (CRP), Common Reflection Surface (CRS), time migration*

ABSTRACT

Since the early days of seismic processing, time migration has proven to be a valuable tool for a number of imaging purposes. Main motivations for its widespread use include robustness with respect to velocity errors, as well as fast turnovers and low computation costs. In areas of complex geology, in which it has well-known limitations, time migration can still be value by providing first images and also attributes, which can be of much help in further, comprehensive depth migration. Time migration is a very close process to the zero-offset common-reflection-surface (ZO CRS) stacking method, in fact, Kirchhoff time migration operators can be readily formulated in terms of CRS parameters. In the nineties, several studies have shown appealing advantages in the use of common-reflection-point (CRP) traveltimes to replace conventional common-midpoint (CMP) traveltimes for a number of stacking and migration purposes. In this paper, we follow that trend and introduce a Kirchhoff-type prestack time migration algorithm, referred to as CRP time migration. The algorithm is based on a CRP operator together with optimal apertures, both computed with the help of CRS parameters. Field data example indicate the good potential of the proposed technique.

INTRODUCTION

Time migration is routinely applied in seismic processing to obtain first, time-domain, images in a fast and inexpensive way. In many situations, typically mild to moderate laterally velocity variations, time migration can yield satisfactory imaging solutions. Advantages of time migration include robustness (less sensitivity to velocity errors), fast turnovers and low computational costs. Losses in image accuracy and interpretation power (mainly associated with geological complexity and strong lateral velocity variations) are well-known limitations of time migration, as compared to comprehensive depth migration (see, e.g., Hubral and Krey, 1980; Yilmaz, 2001; Robein, 2003). Because of noise reduction, collapse of diffractions and triplications, time-migrated images can be of help in event picking, seismic tomography (Dell et al., 2014), as well as time-to-depth conversion (Cameron et al., 2007; Iversen and Tygel, 2008).

The good properties of time migration motivates the search of more accurate algorithms to overcome limitations and enlarge the applicability of time migration. As shown in the literature (Bancroft et al., 1994; Perroud et al., 1999; Spinner and Mann, 2006; Coimbra et al., 2013), it is advantageous to replace the conventional NMO (for CMP stacking) or diffraction (for time migration) operators by appropriate common-reflection-point (CRP) operators, the latter being constructed, typically with common-reflection-surface (CRS) parameters. Moreover, additional accuracy is also obtained by considering minimal, so-called projected Fresnel Zone (PFZ), apertures (Schleicher et al., 1997), such apertures also being estimated using CRS parameters.

In this paper, we follow the trend of performing Kirchhoff-type, time migration under the use of a CRP operator and optimal apertures, both computed with the help of CRS parameters. The approach is called CRP time migration. Besides describing the proposed technique, we briefly discuss the related approaches, already available in the literature. A field data example confirm the good potential of the proposed technique for accurate time migration.

FORMULATION

The CRP time migration technique envisaged here is formulated as a Kirchhoff-type algorithm, in which the migration operator is a CRP traveltime defined in terms of CRS parameters estimated from the prestack data. Furthermore, the same CRS parameters also define a minimal aperture in which the Kirchhoff summation is optimally carried out.

The construction of the proposed CRP time migration is based on the relationships between the traveltime operators of stacking (here represented by the ZO CRS diffraction traveltime) and time migration (here represented by the double-square root (DSR) traveltime), in which both operators refer to the same (unknown) target reflector. For simplicity, we assume that the acquisition surface is planar horizontal.

Notation: Both operators are defined on a same prestack data volume, with traces specified as $(\mathbf{m}, \mathbf{h})$, in which $\mathbf{m} = (m_1, m_2)^T$ and $\mathbf{h} = (h_1, h_2)^T$ represent midpoint and half-offset coordinates. As usual practice, we assume that the application of the stacking operator produces a data volume that well approximates the one obtained when the subsurface is illuminated by a ZO acquisition. In the same way, the application of the time migration operator produces a prestack Kirchhoff time-migrated image of that subsurface.

The central point of the stacking operator (i.e., the point where the stacking output is assigned) is denoted by $(\mathbf{m}_0, t_0)$, in which $\mathbf{m}_0$ represents trace location and t_0 the traveltime in the ZO (stacked) domain. More specifically, t_0 represents the two-way traveltime of the ZO reflection ray (assumed non-converted primary) from the surface point specified by $\mathbf{m}_0$ to the target reflector. That ZO ray is called the central normal ray and supposed to be uniquely determined by $\mathbf{m}_0$. The point where the ZO central ray hits the target reflector is referred to as the normal-incidence point (NIP).

In the same way, the central point of the time migration operator (i.e., the point where the time migration output is assigned) is denoted by $(\mathbf{x}_0, \tau_0)$, in which $\mathbf{x}_0 = (x_1, x_2)^T$ represents trace location and τ_0 is the two-way traveltime in the time migrated domain. The point at the surface specified by $\mathbf{x}_0$ is determined from the central image ray, which is the one that starts at NIP on the target reflector and hits the surface with slowness vector perpendicular to that surface.

Stacking and time migration operators: With the notations described above, we are ready to write the stacking and time migration operators under consideration. We recall that such operators are linked to the same (unknown) target reflector. More specifically, the central ZO points $(\mathbf{m}_0, t_0)$ and $(\mathbf{x}_0, \tau_0)$ of the stacked and time migration operators relates to the same NIP at the target reflector by means of the central ZO and image rays, respectively. We have

(a) Stacking operator: That is given by the ZO CRS diffraction moveout, defined in the prestack domain and central point, $(\mathbf{m}_0, t_0)$ at the ZO (stacked) volume.

$$t^D_{CRS}(\mathbf{m}, \mathbf{h}) = \sqrt{\left[t_0 + \mathbf{a}^T(\mathbf{m} - \mathbf{m}_0)\right]^2 + (\mathbf{m} - \mathbf{m}_0)^T \mathbf{C} (\mathbf{m} - \mathbf{m}_0) + \mathbf{h}^T \mathbf{C} \mathbf{h}}, \tag{1}$$

(b) Time-migration operator: That is given by the double-square-root (DSR) moveout, defined in the prestack domain and of central point $(\mathbf{x}_0, \tau_0)$ in the time-migrated domain

$$\begin{aligned} t_M(\mathbf{m}, \mathbf{h}) &= (1/2)\sqrt{\tau_0^2 + (\mathbf{m} - \mathbf{h} - \mathbf{x}_0)^T \mathbf{S} (\mathbf{m} - \mathbf{h} - \mathbf{x}_0)} \\ &+ (1/2)\sqrt{\tau_0^2 + (\mathbf{m} + \mathbf{h} - \mathbf{x}_0)^T \mathbf{S} (\mathbf{m} + \mathbf{h} - \mathbf{x}_0)} \, . \end{aligned} \tag{2}$$

In the literature, the time-migration quantity, $\mathbf{S}$, is referred to as the *sloth parameter*. For later use, it is convenient to write down the above traveltimes in the ZO configuration, namely $t^D_{ZO}(\mathbf{m}) = t^D_{CRS}(\mathbf{m}, \mathbf{0})$ and $t^M_{ZO}(\mathbf{m}) = t_M(\mathbf{m}, \mathbf{0})$. After a little algebra, we find

$$[t^D_{ZO}(\mathbf{m})]^2 = t_0^2 + 2t_0 \mathbf{a}^T(\mathbf{m} - \mathbf{m}_0) + (\mathbf{m} - \mathbf{m}_0)^T(\mathbf{a}\mathbf{a}^T + \mathbf{C})(\mathbf{m} - \mathbf{m}_0) \, , \tag{3}$$

$$[t^M_{ZO}(\mathbf{m})]^2 = \tau_0^2 + (\mathbf{m} - \mathbf{x}_0)^T \mathbf{S} (\mathbf{m} - \mathbf{x}_0) \, . \tag{4}$$

Relationships between coefficients of stacking and time migration operators: We now investigate the link between the coefficients of the stacking and time migration operators related to the same target reflector. For that, we consider stacking and time-migration ZO operators of Equations (3) and (4) in the main text.

We suppose that the the central point $(\mathbf{m}_0, t_0)$ of the stacking operator is a reflection point in the ZO (stacked) domain and, moreover, that point mapped to $(\mathbf{x}_0, \tau_0)$ after time migration. Following, e. g., Mann et al. (2000) (in the 2D situation) and Gelius and Tygel (2015) (in 3D case), we recall that the time-migrated point, $(\mathbf{x}_0, \tau_0)$, that corresponds to the ZO point $(\mathbf{m}_0, t_0)$, is the minimum (apex) of the stacking operator, $t^D_{ZO}(\mathbf{m})$. As such, that apex, $\mathbf{m} = \mathbf{x}_0$, is determined by the condition

$$\left.\frac{\partial [t^D_{ZO}]^2}{\partial \mathbf{m}}\right|_{\mathbf{m}=\mathbf{x}_0} = 2t^D_{ZO}(\mathbf{x}_0)\left.\frac{\partial t^D_{ZO}}{\partial \mathbf{m}}\right|_{\mathbf{m}=\mathbf{x}_0} = 2[t_0\mathbf{a} + (\mathbf{a}\mathbf{a}^T + \mathbf{C})(\mathbf{x}_0 - \mathbf{m}_0)] = 0\,. \tag{5}$$

Solving for $\mathbf{m}_0$ and substituting into Equation (3), leads to the expressions

$$\mathbf{x}_0 = \mathbf{m}_0 - t_0(\mathbf{a}\mathbf{a}^T + \mathbf{C})^{-1}\mathbf{a}\,, \tag{6}$$

$$\tau_0 = t^D_{ZO}(\mathbf{x}_0) = t_0\sqrt{1 - \mathbf{a}^T(\mathbf{a}\mathbf{a}^T + \mathbf{C})^{-1}\mathbf{a}}\,. \tag{7}$$

Moreover, we also find

$$t^D_{ZO}(\mathbf{m})^2 = \tau_0^2 + (\mathbf{m} - \mathbf{x}_0)^T\left(\mathbf{a}\mathbf{a}^T + \mathbf{C}\right)(\mathbf{m} - \mathbf{x}_0)\,, \tag{8}$$

so that, comparison with the ZO time-migration operator $t^M_{ZO}(\mathbf{m})$ of Equation (4) leads to the additional relations

$$\mathbf{S} = \mathbf{a}\mathbf{a}^T + \mathbf{C}\,, \tag{9}$$

$$t_0^2 = [t^M_{ZO}(\mathbf{m}_0)]^2 = \tau_0^2 + (\mathbf{m}_0 - \mathbf{x}_0)^T\mathbf{S}(\mathbf{m}_0 - \mathbf{x}_0)\,. \tag{10}$$

We also observe that

$$\mathbf{C} = 4\mathbf{V}^{-2}_{NMO}, \quad \text{and} \quad \mathbf{S} = 4\mathbf{V}^{-2}_{M}\,, \tag{11}$$

where $\mathbf{V}_{NMO}$ and $\mathbf{V}_M$ are the so-called NMO and time migration velocity ellipses, evaluated at $(\mathbf{m}_0, t_0)$ and $(\mathbf{x}_0, \tau_0)$, respectively. We note that, in the 2D situation, V_{NMO} and V_M represent the NMO and time migration velocities, respectively.

CRP curve and CRP surface: In what follows, we assume that the quantities $\{\mathbf{m}_0, t_0, \mathbf{a}, \mathbf{C}\}$ are given. That differs from the usual practice with the CRS method, in which the central point, $(\mathbf{m}_0, t_0)$ is given and the CRS parameters $\mathbf{a}$ and $\mathbf{C}$ are estimated from the data and attached to that central point. Here, we the four parameters $\{\mathbf{m}_0, t_0, \mathbf{a}, \mathbf{C}\}$ are all freely given. At a later stage, these four parameters will be estimated regarding their relationship to a given central point $(\mathbf{x}_0, \tau_0)$ in the time-migrated domain.

We recall that the CRP gather that pertains to a given central point, $(\mathbf{m}_0, t_0)$, assumed to be a reflection point in the ZO (stacked) volume, consists of the source-receiver pairs, $(S_{CRP}(\mathbf{h}), G_{CRP}(\mathbf{h}))$ which, for varying half offsets, $\mathbf{h}$, share the same reflection point at the target reflector as the one (NIP) determined by $(\mathbf{m}_0, t_0)$. As shown in Appendix A, the quantities $\{\mathbf{m}_0, t_0, \mathbf{a}, \mathbf{C}\}$, determine the source $S_{CRP}(\mathbf{h}) = \mathbf{m}_{CRP}(\mathbf{h}) - \mathbf{h}$ and receiver $G_{CRP}(\mathbf{h}) = \mathbf{m}_{CRP}(\mathbf{h}) + \mathbf{h}$, in which the midpoints $\mathbf{m}_{CRP}(\mathbf{h})$, is given by

$$\mathbf{m}_{CRP}(\mathbf{h}) = \mathbf{m}_0 + \frac{2(\mathbf{h}^T\mathbf{a})\,\mathbf{h}}{t_0 + \sqrt{t_0^2 + 4(\mathbf{h}^T\mathbf{a})^2}}\,. \tag{12}$$

In the following, the CRP traveltime curve, $t_{CRP}(\mathbf{h})$ (see Figure 1) that refers to the quantities $\{\mathbf{m}_0, t_0, \mathbf{a}, \mathbf{C}\}$ is chosen to be the one that results from the DSR traveltime applied to the CRP gather that corresponds to such quantities. In symbols

$$t_{CRP}(\mathbf{h}) = t_M(\mathbf{m}_{CRP}(\mathbf{h}), \mathbf{h})\,. \tag{13}$$

For varying $\mathbf{m}$ in the neighborhood of $\mathbf{m}_0$ and small varying $\mathbf{h}$, the CRP stacking surface, $T_{CRP}(\mathbf{m},\mathbf{h})$ (see Figure 1) that refers to the central point, $(\mathbf{m}_0, t_0)$, in the ZO (stacked) domain is chosen to be (see Appendix A),

$$T_{CRP}(\mathbf{m},\mathbf{h}) = t_{CRP}(\mathbf{h}) + [\mathbf{a}_{CRP}(\mathbf{h})]^T[\mathbf{m} - \mathbf{m}_{CRP}(\mathbf{h})] \,, \tag{14}$$

with

$$\mathbf{a}_{CRP}(\mathbf{h}) = \frac{\partial t_M}{\partial \mathbf{m}}(\mathbf{m}_{CRP}(\mathbf{h}),\mathbf{h}) \,. \tag{15}$$

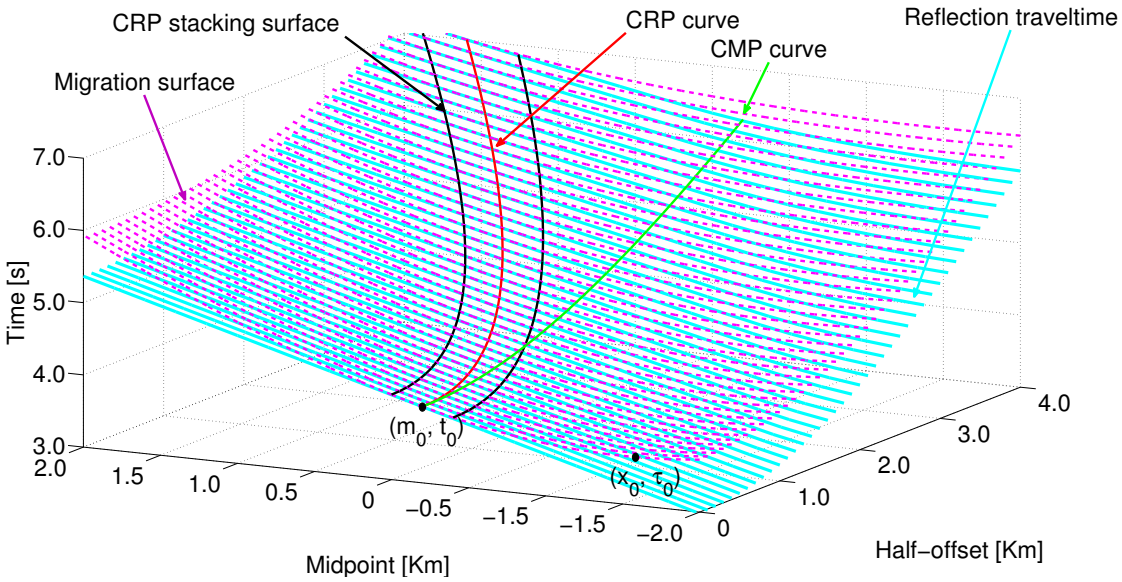

Figure 1: 2D example of a CRP curve computed on (m_0, t_0) for a synthetic dipping plane reflector. Note that the CRP curve follows the migration surface (starting at (x_0, τ_0)) along the offsets and also is tangent to the reflection traveltime (CRP stacking surface). In constrast, the CMP curve was not able maintain this adjustment along the offsets.

CRP TIME MIGRATION ALGORITHM

Our aim now is to apply the previous results to construct a CRP time migration traveltime, $t^M_{CRP} = t^M_{CRP}(\mathbf{h})$, and CRP time migration surface, $T^M_{CRS} = T^M_{CRS}(\mathbf{m},\mathbf{h})$ that refer to a given (central) image point, $(\mathbf{x}_0, \tau_0)$, in the time migration domain. For that, we need to estimate the quantities, $\{\mathbf{m}^M_0, t^M_0, \mathbf{a}_M, \mathbf{C}_M\}$, that pertain to the given $(\mathbf{x}_0, \tau_0)$ in the time-migrated domain.

From Equations (6)-(7), we readily see that

$$\begin{aligned} \mathbf{m}^M_0 &= \mathbf{x}_0 + \tau_0 \left[1 - \mathbf{a}^T_M \mathbf{S}^{-1}_M \mathbf{a}_M\right]^{-1/2} (\mathbf{S}^{-1}_M \mathbf{a}_M) \,, \\ t^M_0 &= \tau_0 \left[1 - \mathbf{a}^T_M \mathbf{S}^{-1}_M \mathbf{a}_M\right]^{-1/2} \,, \end{aligned} \tag{16}$$

where we used the notation

$$\mathbf{S}_M = \mathbf{a}_M \, \mathbf{a}^T_M + \mathbf{C}_M \,. \tag{17}$$

From Equations (16), we readily see that our problem reduces to find the parameter pair $(\mathbf{a}_M, \mathbf{C}_M)$. Once these quantities are obtained, the sought-for CRP curve and surface are given by

$$\begin{aligned} t^M_{CRP}(\mathbf{h}) &= t_{DSR}(\mathbf{m}^M_{CRP}(\mathbf{h}),\mathbf{h}) \,, \\ T^M_{CRP}(\mathbf{m},\mathbf{h}) &= t^M_{CRP}(\mathbf{h}) + [\mathbf{a}^M_{CRP}(\mathbf{h})]^T[\mathbf{m} - \mathbf{m}^M_{CRP}(\mathbf{h})] \,, \end{aligned} \tag{18}$$

where $\mathbf{m}^M_{CRP}$ and $\mathbf{a}^M_{CRP}$ are the same functions as their counterparts $\mathbf{m}_{CRP}$ and $\mathbf{a}_{CRP}$, computed, however, with the quantities $\{\mathbf{m}^M_0, t^M_0, \mathbf{a}_M, \mathbf{C}_M\}$.

Time migration parameter estimation: We are now ready to address the problem of estimating the parameters $\mathbf{a}_M$ and $\mathbf{C}_M$, from which the central point, $(\mathbf{m}^M_0, t^M_0)$, as well as the CRP curve, $t^M_{CRP}(\mathbf{h})$, and CRP surface, $T^M_{CRP}(\mathbf{m}, \mathbf{h})$, are obtained. That is simply done as follows: For a user-selected ensemble of trial parameters $\{\mathbf{a}, \mathbf{C}\}$, construct for each of them the CRP surface, $T_{CRP}(\mathbf{m}, \mathbf{h})$ and compute the stacking energy (semblance) along that surface. The parameter pair for which the maximum energy is attained is the one to be selected.

The estimations indicated above require proper apertures in midpoint and half-offset directions. The aperture in midpoint direction is attached to the estimation of the midpoint inclination, $\mathbf{a}^M_{CRP}$, of the CRP surface for varying offsets. Since $\mathbf{a}$ is the first derivative in midpoint, only a small aperture is needed and experiments. In our 2D experiments, we found that aperture sizes of five traces for each offset are enough. Based on these results, in the 3D case, we recommend the same aperture size in inline and crossline directions (i.e., totaling 25 traces in regular grid for each offset). In offset direction, the aperture should be the same as in any prestack time migration. Thus, in the 3D case, the number of traces considered on each estimation of $\mathbf{a}_M$ and $\mathbf{C}_M$ is the number of midpoint traces times the number of offsets.

Computation of CRP time migration: As earlier indicated, we propose Kirchhoff-type time migration such that, for each output image point, stacks the prestack data along the CRP surface that corresponds to that output point. as stacking migration using the CRP surface that refers to the image point. In analogy of the well-established Kirchhoff depth migration (see, e.g., Schleicher et al., 1993), the CRP time migration is computed by an expression that has the form

$$D^M_{CRP}(\mathbf{x}_0, \tau_0) = -\frac{1}{2\pi} \int_{\mathcal{A}} W^M_{CRP} \left[\partial_t D\right]_{t=t^M_{CRP}} d\mathbf{m} d\mathbf{h} \, . \tag{19}$$

Here, $D^M_{CRP}(\mathbf{x}_0, \tau_0)$ is the time migration output at the image point, $(\mathbf{x}_0, \tau_0)$, $D = D(\mathbf{m}, \mathbf{h}, t)$ is the prestack data. As well known (see, e.g., Schleicher et al., 1993), the partial derivative of the data, $\partial_t D(\mathbf{m}, \mathbf{h}, t)$ with respect to time is applied to preserve the original time shape of the seismic signal. Moreover, $t^M_{CRP} = t^M_{CRP}(\mathbf{m}, \mathbf{h})$ represents the CRP surface that refers to the (output) image point.

The quantity W^M_{CRP} represents the weight function that aims in recovering of the amplitudes. Based on Zhang et al. (2000), we use the true-amplitude weight for a locally homogeneous medium of matrix migration velocity determined by the matrix $\mathbf{S}$ (see Equation (11)),

$$W^M_{CRP} = \frac{\tau_0 \sqrt{\det \mathbf{S}}}{4(\delta_h)^2} \left(\frac{1}{t_S} + \frac{1}{t_G}\right) \left(\frac{t_S}{t_G} + \frac{t_G}{t_S}\right) , \tag{20}$$

to measure the amplitudes stacked along of the diffraction manifold in Equation (19). The values t_S and t_G are defined in (A-2) and (A-3), respectively.

The migration aperture, denoted $\mathcal{A}$ represents the region over which the migration integral is performed. Based on the concept of Projected Fresnel Zone (PFZ) (Schleicher et al., 1997), the aperture $\mathcal{A}$ is proposed to consist of points $(\mathbf{m}, \mathbf{h})$ which simultaneously satisfy the conditions

$$\|\mathbf{m} - \mathbf{m}_{CRP}(\mathbf{h})\| < \delta_m \quad \text{and} \quad \|\mathbf{h}\| < \delta_h \, , \tag{21}$$

where, δ_m and δ_h are midpoint and half-offset aperture bounds. Here, the aperture bound in half-offset direction, δ_h, is taken as the one used in any prestack time migration. Following the same lines as in Faccipieri et al. (2015), the aperture bound in midpoint direction, δ_m can be given by

$$\delta_m = \alpha \sqrt{\frac{w t^M_0}{\lambda_C}} \, , \tag{22}$$

where, $|\lambda_C| = \max\{|\lambda_{C1}|, |\lambda_{C2}|\}$, in which λ_{C1} and λ_{C2} are the eigenvalues of the 2×2 symmetric matrix $\mathbf{C}$, w is the length of the seismic pulse. Moreover, t^0_M is the ZO traveltime that is given by Equation (16), in terms of the CRS parameters, $\{\mathbf{a}_M, \mathbf{C}_M\}$, that pertain to the (output) image point $(\mathbf{x}_0, \tau_0)$. Finally, $\alpha > 1$ is a user-selected adjustment parameter.

2.5D situation: In the case of 2D dataset, the above-described time-migrated algorithm needs to be modified so as to yield 3D meaningful amplitudes after integration on a single seismic line. To overcome this situation, we adopt the so-called 2.5D assumption, which considers that the geological properties of the medium do not vary in the out-of-plane direction of the seismic line, at the same time maintaining the 3D character of a point source and point receiver. In this case, the out-of-plane influence to the amplitudes can be accounted for from in-plane information only. More information on 2.5D media can be found in, e.g., Bleistein (1986). In 2D seismic data, the parameters $\mathbf{a}$ and $\mathbf{C}$ become the scalars, having the form

$$a = \mathbf{a}^T \mathbf{u}_\theta \quad \text{and} \quad C = \mathbf{u}_\theta^T \mathbf{C} \mathbf{u}_\theta \tag{23}$$

with

$$\mathbf{u}_\theta = (\cos\theta, \sin\theta)^T , \tag{24}$$

where θ is the acquisition azimuth. The midpoint and offsets coordinates also changes with the azimuth and are given by

$$\mathbf{m} = m\mathbf{u}_\theta \quad \text{and} \quad \mathbf{h} = h\mathbf{u}_\theta. \tag{25}$$

In the 2.5D situation, the CRP time migration integral, Equation (19), becomes

$$D^M_{CRP}(\mathbf{x}_0, \tau_0) = \frac{1}{\sqrt{2\pi}} \int_{\mathcal{A}} W^M_{2.5D} \left[\partial_t^{1/2} D\right]_{t=t^M_{CRP}} dmdh \tag{26}$$

where the operator $\partial_t^{1/2}$ represents the anti-causal half-derivative in time (see. e.g., Bleistein, 1986). For the weight function, Equation (20), we use the expression derived on Zhang et al. (2000), namely

$$W^M_{2.5D} = \frac{\tau_0}{2\delta_h} \sqrt{\frac{1}{t_S} + \frac{1}{t_G}} \left(\frac{t_S}{t_G} + \frac{t_G}{t_S}\right) . \tag{27}$$

The aperture bound in midpoint is now given by (compare with Equation (22) for the 3D case)

$$\delta_m^{2.5D} = \alpha \sqrt{\frac{w t_0^M}{C}} . \tag{28}$$

The aperture bound in half-offset, δ_h is, once more, the one used in any time-migration algorithm.

EXAMPLES

The proposed CRP time migration was applied to a 2D real dataset acquired offshore in Brazil at Jequitinhonha basin. The dataset has 4 ms time sampling, 12.5 m between Common Midpoint (CMP) gathers, 25 m between hydrophones with minimum and maximum offsets of 150 m and 3125 m, respectively. For comparison purposes, Figure 2 (left) shows a CRS stacked section obtained with global estimation of parameters with the following apertures: (i) Midpoint: 30 m from zero to 1.3 s, increasing linearly until 150 m at 3.5 s and constant until the maximum time sample. (ii) Offset: 650 m from 0 to 1.3 s, increasing linearly until 1050 m at 3.5 s and constant until the final time, 6.0 s. A conventional post-stack Kirchhoff time-migrated section constructed with that dataset is shown at Figure 2 (right). The migration aperture that has been used was ten times greater than the minimum aperture proposed, $\alpha = 10$ in Equation (28). We observe that, under that conventional procedure, smaller apertures were not able to image some of the dips present in the data. To carry out the CRP time migration, the CRS parameters a and C must be estimated using T^M_{CRP} from Equation (18). In the present example, the estimations were performed using constant midpoint and half-offset apertures of 50 m and 1000 m, respectively. Once these parameters were estimated, for each (x_0, τ_0), the dataset was migrated, considering the 2.5D case formulation, given by Equations (26)-(27). The obtained time-migration section is shown in Figure 3 (left). The migration apertures were calculated using Equation (28) for each (m_0^M, t_0^M) with $\alpha = 1$ and $w = 40$ ms which leads to different values of apertures depending of C_M and t_0^M. Figure 3 (right) shows the semblance values for the estimated parameters. It is possible to identify and quantify the regions where the CRP surface adjusted the events properly. The semblance panel can be seen as valuable tool for the purposes of evaluation and quality control of the CRP time migration.

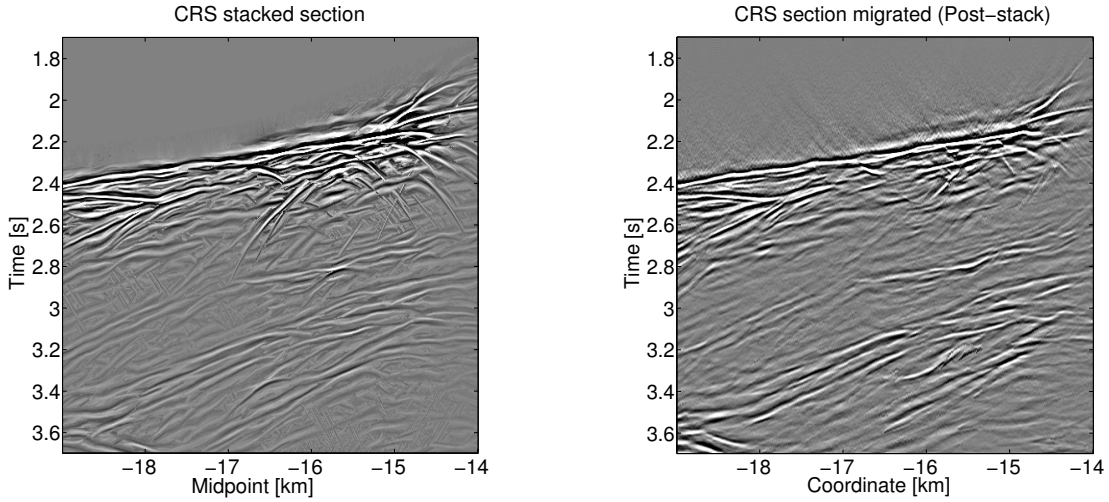

Figure 2: Stacked section obtained with CRS method (left) and its post-stack Kirchhoff migration with aperture ten times greater ($\alpha = 10$) than the proposed minimum aperture in midpoints (right). Remark: The velocity model used to migrate the dataset was obtained by the CRP time migration.

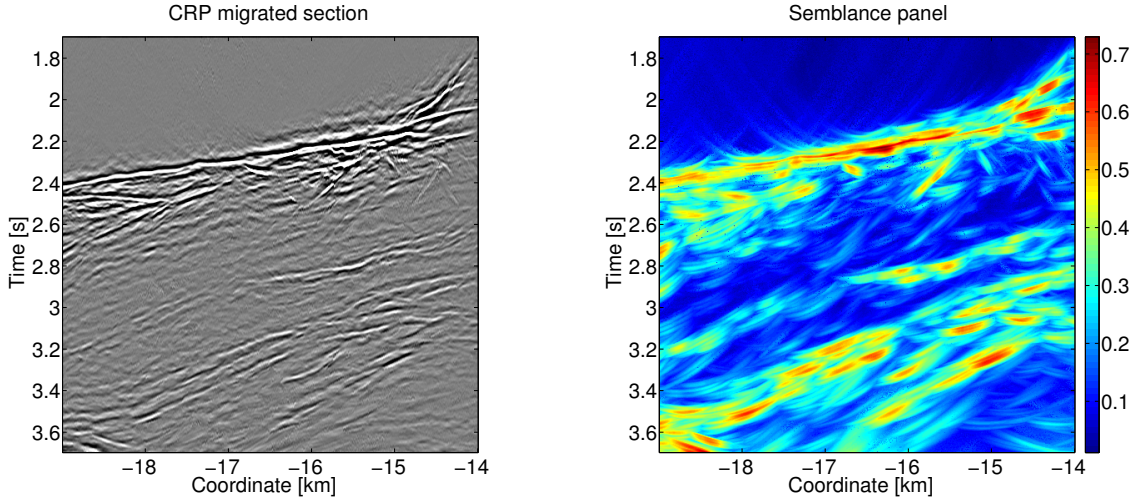

Figure 3: Left: Prestack time-migrated section obtained with the proposed CRP algorithm using the minimum apertures in midpoint. Right: Semblance obtained on the estimation of parameters for each (x_0, τ_0).

Using the same velocity model estimated before, two conventional prestack Kirchhoff time migration were perfomed varying only the migration apertures aiming to examinate their influence on final result. Figure 4 shows theses migrated sections with $\alpha = 1$ (left) and with $\alpha = 10$ (right). For the minimum migration aperture, $\alpha = 1$, some of the dips were not imaged and the reflections appear unfocused. This is expected since the conventional time migration is not able to indentify the region where the constructive interference occurs. In practice, larger migration apertures are used to avoid this limitation. Figure 4 (right) shows an example where the migration aperture was ten times greater and it is possible to observe that the features present on Figure 3 (left) were imaged. However, the noise levels between these two results are considerable which justifies the application of the proposed method.

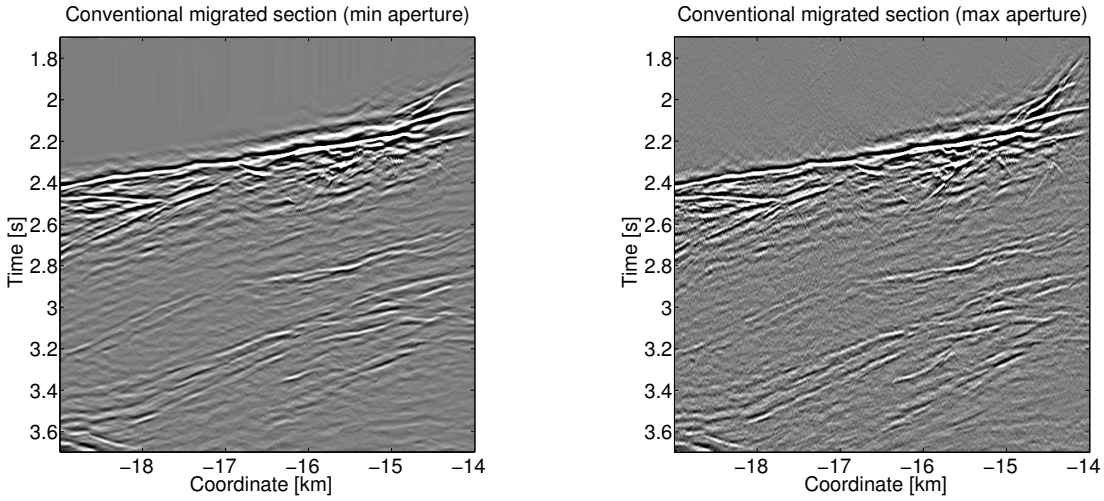

Figure 4: Left: Prestack migrated section obtained with conventional Kirchhoff time migration using the minimum aperture in midpoints, $\alpha = 1$. Right: Same procedure using $\alpha = 10$.

CONCLUSIONS

A Kirchhoff-type, time migration algorithm is proposed that is optimal in two respects. First, the summation is performed along the common-reflection-point (CRP) curve (as opposed to the conventional diffraction-time hyperbola). Second, a small aperture, associated to the projected Fresnel zone (PFZ), is employed that is able to restrict the summation to that part of the CRP curve where constructive interference occurs. A key feature of the algorithm is a transformation function that maps each given image point into a corresponding point in the ZO (stacked) volume and also computes the zero-offset (ZO) common-reflection-surface (CRS) parameters there. Such quantities are used to construct the CRP curve and the summation aperture at each image point. First field-data examples confirm the good potential of the new technique for high-quality, time migration results.

ACKNOWLEDGMENTS

We acknowledge support from the National Council for Scientific and Technological Development (CNPq-Brazil), the National Institute of Science and Technology of Petroleum Geophysics (ICTP-GP-Brazil) and the Center for Computational Engineering and Sciences (Fapesp/Cepid # 2013/08293-7-Brazil). We also acknowledge support of the sponsors of the Wave Inversion Technology (WIT) Consortium.

REFERENCES

Bancroft, J. C., Geiger, H. D., Foltinek, D., and Wang, S. (1994). Prestack migration by equivalent offsets and CSP gathers. In *CREWES Research Report*, volume 6.

Bleistein, N. (1986). Two-and-one-half dimensinal in-plane wavepropagation. *Geophysical Prspecting*, 34:686–703.

Cameron, M. K., Fomel, S. B., and Sethian, J. A. (2007). Seismic velocity estimation from time migration. *Inverse Problems*, 23:1329–1369.

Coimbra, T. A., Novais, A., and Schleicher, J. (2013). Theory of offset-continuation trajectory stack. In *13th International Congress of the Brazilian Geophysical Society & EXPOGEF, Rio de Janeiro, Brazil, 26–29 August 2013*. Society of Exploration Geophysicists and Brazilian Geophysical Society.

Dell, S., Gajewski, D., and Tygel, M. (2014). Image ray tomography. *Geophysical Prospecting*, 62(3):413–426.

Faccipieri, J. H., Coimbra, T. A., Gelius, L.-J., and Tygel, M. (2015). Stacking apertures and estimation strategies for reflection and diffraction enhancement. *Wave Inversion Technology (WIT) Report*, 18.

Gelius, L.-J. and Tygel, M. (2015). Migration-velocity building in time and depth from 3D (2D) common-reflection-surface (CRS) stacking - theoretical framework. *Studia Geophysica et Geodaetica: Accepted for publication*.

Hubral, P. and Krey, T. (1980). *Interval Velocities from Seismic Reflection Time Measurements*. SEG.

Iversen, E. and Tygel, M. (2008). Image-ray tracing for joint 3D seismic velocity estimation and time-to-depth conversion. *Geophysics*, 73(3):S99–S114.

Mann, J., Hubral, P., Traub, B., Gerst, A., and Meyer, H. (2000). *Macro-model independent approximative prestack time migration*. 62nd Mtg. Eur. Assn. Geosci. Eng. EAGE, Expanded Abstracts.

Perroud, M., Hbral, P., and Höcht, G. (1999). Common-reflection-point stacking in laterally inhomogeneous media. *Geophysical Prospecting*, 47:1–24.

Robein, E. (2003). *Velocities, time-imaging and depth-imaging in reflection seismics: Principles and methods*. EAGE.

Schleicher, J., Hubral, P., Tygel, M., and Jaya, M. S. (1997). Minimum apertures and Fresnel zones in migration and demigration. *Geophysics*, 62(1):183–194.

Schleicher, J., Tygel, M., and Hubral, P. (1993). 3-D true-amplitude finite-offset migration. *Geophysics*, 58(8):1112–1126.

Spinner, M. and Mann, J. (2006). True-amplitude based Kirchhoff time migration for AVO/AVA analysis. *Geophysics*, 15:133–152.

Yilmaz, O. (2001). *Seismic Data Analysis: Processing, Inversion and Interpretation of Seismic Data (2nd edition)*. Society of Exploration Geophysicists (SEG), Oklahoma, Tulsa, USA.

Zhang, Y., Gray, S., and Young, J. (2000). Exact and approximate weights for Kirchhoff migration. In *SEG Technical Program Expanded Abstracts 2000*. Society of Exploration Geophysicists.

APPENDIX A

EXPRESSION OF CRP TRAJECTORY

We now focus our attention on the construction of the CRP operator that refers to a given time-migration sloth parameter, $\mathbf{S}$ and time-migration central point, $(\mathbf{x}_0, \tau_0)$. For that, start with the time migration operator of Equation (2) for a fixed half-offset, which we recast in the more convenient form

$$t_M(\mathbf{m}, \mathbf{h}; \mathbf{x}_0, \tau_0) = t_S(\mathbf{m}, \mathbf{h}; \mathbf{x}_0, \tau_0) + t_G(\mathbf{m}, \mathbf{h}; \mathbf{x}_0, \tau_0)\,, \tag{A-1}$$

with $t_S = t_S(\mathbf{m}, \mathbf{h}; \mathbf{x}_0, \tau_0)$ and $t_G = t_G(\mathbf{m}, \mathbf{h}; \mathbf{x}_0, \tau_0)$ given by

$$t_S^2 = \frac{\tau_0^2}{4} + \frac{1}{4}(\mathbf{m} - \mathbf{h} - \mathbf{x}_0)^T \mathbf{S}(\mathbf{m} - \mathbf{h} - \mathbf{x}_0)\,, \tag{A-2}$$

$$t_G^2 = \frac{\tau_0^2}{4} + \frac{1}{4}(\mathbf{m} + \mathbf{h} - \mathbf{x}_0)^T \mathbf{S}(\mathbf{m} + \mathbf{h} - \mathbf{x}_0)\,. \tag{A-3}$$

Note the change in notation in the above expressions, in which the dependence on the time-migration central point, $(\mathbf{x}_0, \tau_0)$, is made explicitly. Introducing the notation $\Delta\mathbf{m} = \mathbf{m} - \mathbf{m}_0$ and also using Equation (10) to replace τ_0^2 in Equations (A-2) and (A-3), we can recast the time-migration traveltime, $t_M(\mathbf{m}, \mathbf{h}; \mathbf{x}_0, \tau_0)$, of Equation (A-1) into the modified form, more convenient to our purposes,

$$t_M^{(\mathbf{m}_0, t_0)}(\mathbf{m}, \mathbf{h}; \mathbf{x}_0) = t_S^{(\mathbf{m}_0, t_0)}(\mathbf{m}, \mathbf{h}; \mathbf{x}_0) + t_G^{(\mathbf{m}_0, t_0)}(\mathbf{m}, \mathbf{h}; \mathbf{x}_0)\,, \tag{A-4}$$

where

$$4[t_S^{(\mathbf{m}_0,t_0)}]^2(\mathbf{m},\mathbf{h};\mathbf{x}_0) = t_0^2 + (\Delta\mathbf{m}-\mathbf{h})^T\mathbf{S}(\Delta\mathbf{m}-\mathbf{h}) + 2(\mathbf{m}_0-\mathbf{x}_0)^T\mathbf{S}(\Delta\mathbf{m}-\mathbf{h})\,, \tag{A-5}$$

$$4[t_G^{(\mathbf{m}_0,t_0)}]^2(\mathbf{m},\mathbf{h};\mathbf{x}_0) = t_0^2 + (\Delta\mathbf{m}+\mathbf{h})^T\mathbf{S}(\Delta\mathbf{m}+\mathbf{h}) + 2(\mathbf{m}_0-\mathbf{x}_0)^T\mathbf{S}(\Delta\mathbf{m}+\mathbf{h})\,. \tag{A-6}$$

Geometrical interpretation of $t_M^{(\mathbf{m}_0,t_0)}(\mathbf{m},\mathbf{h};\mathbf{x}_0)$: The time-migration traveltime of Equations (A-4)-(A-6) admit the following appealing interpretation: Consider the isochrone in depth domain specified by the central point $(\mathbf{m}_0,t_0)$. That isochrone is taken only conceptually because we do not have a depth-velocity model. For any point, P, on that isochrone, specified by the lateral coordinate, $\mathbf{x}_0$, and for every fixed half-offset, $\mathbf{h}$, Equation (A-4) represents the (DSR) traveltime that refers to the point diffractor the P under common-offset configuration of half-offset, $\mathbf{h}$.

For varying point diffractors along the isochrone (as specified by correspondingly varying coordinate vectors, $\mathbf{x}_0$, an ensemble of diffraction surfaces are obtained. Such ensemble has, as an envelope, the reflection response of the isochrone, taken as a reflector, also under the same common-offset configuration specified by $\mathbf{h}$. In order to determine the envelope of the ensemble of diffraction surfaces parameterized by $\mathbf{x}_0$, We apply the so-called envelope condition

$$\frac{\partial t_M}{\partial \mathbf{x}_0}(\mathbf{m},\mathbf{h}) = \mathbf{0}\,. \tag{A-7}$$

In view of the expressions

$$\begin{aligned}\frac{\partial t_S^2}{\partial \mathbf{x}_0} &= 2t_S\frac{\partial t_S}{\partial \mathbf{x}_0} = -\mathbf{S}(\Delta\mathbf{m}-\mathbf{h})\,,\\ \frac{\partial t_G^2}{\partial \mathbf{x}_0} &= 2t_G\frac{\partial t_G}{\partial \mathbf{x}_0} = -\mathbf{S}(\Delta\mathbf{m}+\mathbf{h})\,.\end{aligned} \tag{A-8}$$

Using Equation (A-8) in Equation (A-7), leads to

$$\frac{1}{t_S}\mathbf{S}(\Delta\mathbf{m}-\mathbf{h}) + \frac{1}{t_G}\mathbf{S}(\Delta\mathbf{m}+\mathbf{h}) = \mathbf{0}\,, \tag{A-9}$$

which transforms into

$$t_G(\Delta\mathbf{m}+\mathbf{h}) = -t_S(\Delta\mathbf{m}-\mathbf{h})\,. \tag{A-10}$$

Squaring both sides of the above equation and after a little algebra, we obtain

$$\mathbf{x}_0 = \mathbf{m}_0 + \frac{4t_0^2\mathbf{S}^{-1}\Delta\mathbf{m}}{\mathbf{h}^T\mathbf{h}-\Delta\mathbf{m}^T\Delta\mathbf{m}}\,. \tag{A-11}$$

Substitution of Equation (A-11) into Equations (A-5) and (A-6), we find the expression

$$[t_{ISO}^R(\mathbf{m},\mathbf{h};\mathbf{m}_0,t_0)]^2 = \mathbf{h}^T\mathbf{S}\mathbf{h} + \frac{t_0^2\mathbf{h}^T\mathbf{h}}{\mathbf{h}^T\mathbf{h}-\Delta\mathbf{m}^T\Delta\mathbf{m}}\,. \tag{A-12}$$

Geometrical interpretation of $t_{ISO}^R(\mathbf{m},\mathbf{h})$: Consider a fixed half-offset, $\mathbf{h}$. Equation (A-12) represents the reflection traveltime of the ZO isochrone that refers to the central point, $(\mathbf{m}_0,t_0)$, taken as a depth reflector, under the common-offset configuration of that fixed half-offset. Let us suppose now that the ZO reflection traveltime of the target reflector is given by the expression $t_0 = t_0(\mathbf{m}_0)$. For varying points $(\mathbf{m}_0,t_0(\mathbf{m}_0))$ on that reflection curve, the traveltime functions of Equation (A-12) constitute an ensemble of reflection traveltimes of isochrones, parameterized by the midpoints, $\mathbf{m}_0$. The envelope of that ensemble is obtained by the condition

$$\frac{\partial t_{ISO}^R}{\partial \mathbf{m}_0}(\mathbf{m},\mathbf{h};\mathbf{m}_0,t_0) = 0\,. \tag{A-13}$$

Under the consideration that

$$\frac{\partial t_{ISO}^{R}}{\partial \mathbf{m}_0} = \frac{1}{2t_{ISO}^{R}} \frac{\partial [t_{ISO}^{R}]^2}{\partial \mathbf{m}_0} \,, \tag{A-14}$$

we find

$$2\mathbf{a}(\mathbf{h}^T\mathbf{h} - \Delta\mathbf{m}^T\Delta\mathbf{m}) + t_0\Delta\mathbf{m} = \mathbf{0}. \tag{A-15}$$

The above quadratic equation in $\Delta\mathbf{m} = \Delta\mathbf{m}_{CRP} = \mathbf{m}_{CRP} - \mathbf{m}_0$, which $\mathbf{m}_{CRP}$ is given by Equation (12) in the main text.